Ornstein-Zernike equations and simulation results for hard-sphere fluids adsorbed in porous media

Enrique Lomba,* James A. Given,† and George Stell
Department of Chemistry, State University of New York at Stony Brook, Stony Brook, New York 11794-3400

Jean Jacques Weis and Dominique Levesque
Laboratoire de Physique Théorique et Hautes Energies, Bâtiment 211, Université de Paris-Sud, 91405 Orsay CEDEX, France
(Received 28 January 1993)

In this paper we solve the replica Ornstein-Zernike (ROZ) equations in the hypernetted-chain (HNC), Percus-Yevick (PY), and reference Percus-Yevick (RPY) approximations for partly quenched systems. The ROZ equations, which apply to the general class of partly quenched systems, are here applied to a class of models for porous media. These models involve two species of particles: an annealed or equilibrated species, which is used to model the fluid phase, and a quenched or frozen species, whose excluded-volume interactions constitute the matrix in which the fluid is adsorbed. We study two models for the quenched species of particles: a hard-sphere matrix, for which the fluid-fluid, matrix-matrix, and matrix-fluid sphere diameters σ_{11}, σ_{00}, and σ_{01} are additive, and a matrix of randomly overlapping particles (which still interact with the fluid particle as hard spheres) that gives a "random" matrix with interconnected pore structure. For the random-matrix case we study a ratio σ_{01}/σ_{11} of 2.5, which is a demanding one for the theories. The HNC and RPY results represent significant improvements over the PY result when compared with the Monte Carlo simulations we have generated for this study, with the HNC result yielding the best results overall among those studied. A phenomenological percolating-fluid approximation is also found to be of comparable accuracy to the HNC results over a significant range of matrix and fluid densities. In the hard-sphere matrix case, the RPY is the best of the theories that we have considered.

PACS number(s): 61.20.Gy, 61.20.Ja, 47.55.Mh

I. INTRODUCTION

This paper is part of an ongoing project [1] of extending the methods of liquid-state physics (integral equations, renormalized perturbation theory, etc.) to apply to continuum systems with quenched disorder. Such systems include engineering composites, porous materials, gels, amorphous materials, spin glasses, etc. Many such materials can be regarded as being constructed from successively quenched layers, each layer being added to those already in place and allowed to equilibrate, then frozen in place before the next layer is added. The simplest such system consists of just two layers or fractions, one quenched and one annealed. The basic idea is that the particles in the quenched fraction constitute a disordered matrix through which the particles in the annealed fraction move.

A simple mixture of this kind, in which quenched and annealed particles possess only excluded-volume interactions, has already been studied as a model for the properties of fluid adsorbed in a microporous material in papers by Madden and Glandt [2], Madden [3], and Fanti, Glandt, and Madden [4]. The quenched species of immobile particles in the mixtures considered in [2] are assumed to have been formed by a quench from an equilibrium distribution; that is, their distribution represents a realization of an equilibrium ensemble equilibrated in the absence of the mobile (annealed) particles. In [2] Madden and Glandt present both Mayer expansions and integral equations for the properties of such systems. In [3] Madden generalized the formalism of [2] to the case in which the quenched distribution is essentially arbitrary and in [4], Fanti, Glandt, and Madden obtained numerical results in the Percus-Yevick (PY) approximation.

In earlier work [5], two of the authors (J.G. and G.S.) pointed out that the Ornstein-Zernike equations given in [3] (and in the earlier [2]) are not the exact Ornstein-Zernike equations associated with the cluster expansions therein. Instead they correspond to an approximation in which a certain class of terms is neglected in the cluster expansion of the direct correlation function for annealed particles. We shall refer to this as the Madden-Glandt (MG) approximation. In Refs. [1] and [5], a set of coupled integral equations were developed that are exactly satisfied by the correlation functions of a partly quenched system. We call these equations the replica Ornstein-Zernike (ROZ) equations. Several closures to these equations were suggested and discussed in [1] and [5], including some that seem especially appropriate for the porous media models already described. The MG approximation, in particular, proves to be a natural one in the context of the ROZ approach as well as an interaction site approach [6].

The purpose of this paper is to test the results of various closures of the ROZ equations against extensive numerical simulations of these models of porous media. We

want to contribute to understanding the limits of validity of various closures to the ROZ equations; this is a necessary part of a systematic theory of partly quenched media.

This paper is organized as follows. In Sec. II we state the ROZ equations, which are the Ornstein-Zernike equations for partly quenched systems. We motivate these equations, but do not repeat the derivation given in [1] and [5] here. In Sec. III we develop a number of closure conditions for these equations. We emphasize those expected to be of special value for systems involving a molecular liquid adsorbed in a microporous medium. In Sec. IV we discuss numerical algorithms which we have found effective at solving the ROZ equations even at high densities of matrix and/or fluid particles. In Sec. V we discuss the procedure for studying adsorbed-fluid problems by Monte Carlo simulation. We discuss in detail the results of our Monte Carlo simulations, comparing them to numerical solution of the various approximate closures of the ROZ equations developed earlier. We also include a technical Appendix.

II. THE REPLICA ORNSTEIN-ZERNIKE EQUATIONS

In this section we state the replica Ornstein-Zernike (ROZ) equations. Several natural closures for them will be presented in Sec. III.

The ROZ equations are a set of coupled integral equations satisfied by the correlation functions of a partly quenched system. In Refs. [1] and [5] we sketch the derivation of these equations by mapping a partly quenched system onto a limiting case of an equilibrium system (called the replicated system) and considering the standard Ornstein-Zernike equations for the latter. We give further details and discussion in Ref. [7]. We will not repeat the derivation here, but will instead discuss the intuitive meaning of these equations. We consider here a two-species system in which the species-0 particles are quenched or frozen in place and the species-1 particles are annealed or allowed to equilibrate. We will refer to the species-0 particles as matrix particles and species-1 particles as fluid particles. Species-1, i.e., fluid particles are taken to have hard-sphere interactions of range σ_{11} with each other and hard-sphere interactions of range σ_{10} with the matrix particles. There are two natural choices for the potential $v_{00}(r)$ between matrix particles. Taking the matrix particles to be hard spheres is one of them. The simplest case is one of additive diameters, $2\sigma_{10} = \sigma_{11} + \sigma_{00}$. If the matrix particles are large, this gives a model for a porous medium composed of consolidated grains. (If the matrix particles are smaller, impenetrable particles, this gives a model for the short-time response of a suspension.) On the other hand, taking the matrix particles to be spheres that freely overlap each other, but are still impenetrable to fluid particles, gives a well-studied porous-media model with a highly nontrivial pore structure (the case of randomly centered spheres, which we shall refer to as the random-matrix case). We will consider examples of both choices: one in which the matrix particles are randomly centered, and one in which they have a hard-sphere repulsion with range σ_{11} and $\sigma_{00} = \sigma_{10} = \sigma_{11}$.

In discussing the correlation functions of partly quenched media, it is natural to separate the fluid-fluid total correlation function $h_{11}(r)$ into two parts as follows:

$$h_{11}(12) = h_c(12) + h_b(12). \tag{2.1}$$

Here the functions $h_c(r)$ and $h_b(r)$, which we call the connected and blocked functions, respectively, are the natural basis set both for stating the ROZ equations and for discussing their closures. These functions are defined in terms of subsets of the Mayer graphs contributing to $h_{11}(r)$ [2, 3, 8]. The graphs in $h_{11}(r)$ such that the two root points are connected by at least one path of bonds and vertices that includes only ρ_1 vertices contribute to $h_c(r)$. The remainder of the graphs contribute to $h_b(r)$. The connected function $h_c(r)$ accounts for correlations between a pair of fluid particles that are transmitted through successive layers of fluid particles; the blocked function $h_b(r)$ accounts for correlations between fluid particles "blocked" or separated from each other by matrix particles. (We note that even though the matrix particles are immobile, they tend to order the fluid particles on either side of them and thus are capable of mediating correlations "through" a layer of matrix particles.) At very low matrix porosities, i.e., very high densities of matrix particles, the volume accessible to fluid particles is divided into small cavities, each totally surrounded by matrix particles. In this limit, the function $h_c(r)$ describes correlations between fluid particles in the **same** cavity; the function $h_b(r)$ describes correlations between particles in **different** cavities. We make a similar separation of the direct correlation function,

$$c_{11}(12) = c_c(12) + c_b(12). \tag{2.2}$$

We can then write the exact ROZ equations as

$$h_{00} = c_{00} + \rho_0 c_{00} \otimes h_{00}, \tag{2.3}$$

$$h_{10} = c_{10} + \rho_0\, c_{10} \otimes h_{00} + \rho_1\, c_c \otimes h_{10}, \tag{2.4}$$

$$h_{11} = c_{11} + \rho_0\, c_{10} \otimes h_{01} + \rho_1\, c_c \otimes h_{11} + \rho_1\, c_b \otimes h_c, \tag{2.5}$$

$$h_c = c_c + \rho_1\, c_c \otimes h_c \tag{2.6}$$

where, by symmetry, $c_{01} = c_{10}$ and $h_{01} = h_{10}$. Here the symbol $\otimes$ denotes a convolution.

An alternative equation for h_{01} that can be derived from (2.2)–(2.6) is

$$h_{01} = c_{01} + \rho_0 c_{00} \otimes h_{01} + \rho_1 c_{01} \otimes h_c. \tag{2.7}$$

When c_{00}, c_{01}, c_{11}, c_c, and the $\{\rho_i\}$ are prescribed, (2.2)–(2.6) are a closed set of equations for h_{00}, h_{01}, h_{11}, and h_c.

III. APPROXIMATE CLOSURES FOR POROUS-MEDIA MODELS

As noted in [1] there is a class of approximate closures of the ROZ equations that imply the approximation $c_b(r) = 0$, which was used explicitly in [1–4], and which we call the Madden-Glandt (MG) approximation. This class of closures includes the Percus-Yevick (PY) closure, $c_{ij} = f_{ij}y_{ij}$, where f_{ij} is the Mayer function, and the cavity function y_{ij} is defined by the equation $g_{ij} = (1 + f_{ij})y_{ij}$.

We shall begin our discussion with the special case of a random matrix in which the fluid particles interact with the matrix but not with each other. Thus $\sigma_{00} = \sigma_{11} = 0$, $\sigma_{10} \neq 0$. This is the quenched-annealed version of the Widom-Rowlinson model [9]. It is also a simple off-lattice version of the Lorentz gas [10]. Because of the choice of interactions in this model, one can exactly solve for the correlation functions. One finds immediately that $h_{00} = c_{00} = 0$. The only Mayer graphs that contribute to the function $c_{11}(r)$ are those diagrams containing two fluid-particle root points and two or more quenched-particle field points, each joined directly to each of the two root points whereas $c_{10}(r)$ is just $f_{10}(r)$. Using techniques that are standard in Mayer theory, one can sum this class of diagrams to give

$$c_b(12) = \exp[\rho_0 O^o] - 1 - \rho_0 O^o, \tag{3.1}$$

where $O^o(12)$ is the "overlap volume" integral

$$O^o(12) = \int d3\, f_{10}(13) f_{01}(32). \tag{3.2}$$

We have also $c_c(r) = 0$ and

$$h_c(r) = 0. \tag{3.3}$$

There are no annealed paths at all in this model because the bond $f_{11}(r) = 0$. Thus $c_{11} = c_b$ and $h_{11} = h_b$ and the entire contribution to $c_{11}(r)$ comes from graphs ignored by the MG approximation. Equations (2.4) and (2.7) reduce easily to $h_{10} = c_{10}$. But from its Mayer expansion, c_{10} is just f_{10}, so

$$h_{10} = c_{10} = f_{10}, \tag{3.4}$$

while (2.5), when (3.4) is used, reduces to

$$h_{11} = c_{11} + \rho_0 f_{10} \otimes f_{01}. \tag{3.5}$$

From (3.1) and (3.5), the hypernetted-chain (HNC) closure,

$$c_{ij} = -\beta v_{ij} + h_{ij} - \ln g_{ij}, \tag{3.6}$$

is trivially satisfied for $i = 0, 1$ and $j = 0, 1$. It is interesting that this version of the Widom-Rowlison model, in which one of the species is quenched, can be exactly treated so simply, while the fully equilibrated Widom-Rowlinson mixture cannot be [9].

We now generalize this model by including a hard-sphere excluded-volume interaction between the fluid particles, with the other interactions as before, so that it remains a random-matrix model. The resulting model is no longer exactly solvable. However, in the $\rho_1 \to 0$ limit, (3.1) is still exact, as is the HNC approximation. This limit describes the case in which any finite number (for example, two) fluid particles are in a matrix of infinite extent, and it represents a natural reference system for the porous-medium problem.

Physically, the contribution (3.1) of c_b to h_{11} represents a reinforcement or cooperative effect of the overlapping inclusions that make up the porous matrix. When σ_{01} is significantly larger than σ_{11}, such reinforcement is very substantial for the intermediate to high densities of matrix inclusions that characterize many microporous materials. At low density ρ_1 of adsorbed fluid, this contribution to h_{11} from c_b is the dominant one. At higher fluid densities, the $\rho_1 c_b \otimes h_c$ of (2.5) turns out to be a competing term that tends to cancel the c_b term more and more completely as ρ_1 increases, so that the PY approximation (in which both the c_b and the $\rho_1 c_b \otimes h_c$ contributions are neglected) is quite good when ρ_1 is substantial, even for $\sigma_{01} > \sigma_{11}$.

When the matrix consists of particles that are hard spheres with respect to one another (with $\sigma_{00} + \sigma_{11} = 2\sigma_{10}$) the $\rho_1 \to 0$ limit remains a useful one, which describes an equilibrium system of hard spheres of diameter σ_{00} plus a finite number of "tracer" hard-sphere particles of diameter σ_{11} and zero density ρ_1. This reference system is particularly simple when $\sigma_{11} = \sigma_{00}$ since it is then just a one-species hard-sphere system at density ρ_0.

A. HNC-type approximations

We first consider approximations of the HNC type. There are two reasons for expecting these to be accurate for describing matrices formed by freely overlapping particles. The first is that the HNC is exact for noninteracting fluid particles and also for interacting fluid particles in the low fluid-density limit. The second reason for expecting the HNC to have a wide range of validity for calculating the correlation functions of a fluid in a random matrix is that this same approximation has been found to be quite accurate in calculating the material correlation functions for this system [11]. The material correlation functions are the standard quantities used to incorporate the statistics of porous media into the calculations of their bulk properties, for example their permeability to fluid flow. These functions are basically the correlation functions of two tracer particles immersed in a many-body system of the inclusions which make up the matrix. Because tracer particles by definition are at "zero density," the diagram summation leading to Eq. (3.1) is exact also for these functions. Here again this "zero-density" approximation is found to have a wide range of validity [11].

The reference HNC closure has the general form

$$c_{ij}(r) = h_{ij}(r) - \ln[1 + h_{ij}(r)] - \beta v_{ij}(r) + b_{ij}(r) \tag{3.7}$$

for $(i,j) = (0,1)$ or (1,1). Here v_{ij} is the pairwise potential interaction between species i and j particles. The functions $\{b_{ij}\}$ are called bridge functions; they are to be approximated by using the bridge functions from a simpler, reference system. If this is taken to be the ideal gas the bridge function is simply zero, and therefore the reference HNC reduces to the standard HNC approach. For the matrix models considered here, these can be rewritten

$$c_{ij}(12) = \begin{cases} -1 - \gamma_{ij}(12) & \text{if } r < \sigma_{ij} \\ \exp\left[-\beta v_{ij}(r) + \gamma_{ij}(12) + b_{ij}(r)\right] - 1 - \gamma_{ij}(12) & \text{if } r \geq \sigma_{ij}\ , \end{cases} \tag{3.8}$$

where (i,j) is $(1,0)$ or $(1,1)$, and $\gamma_{ij}(r) = h_{ij}(r) - c_{ij}(r)$. Also

$$c_b(12) = \exp\left[\gamma_b(12) + b_b(r)\right] - 1 - \gamma_b(12). \tag{3.9}$$

This latter equation represents the HNC closure that comes out of the ROZ equations, in which (before one takes the replica limit) c_b represents correlation between two noninteracting replicas of the same fluid particle.

For the random matrix, the reference HNC is simply the ordinary HNC, as already noted. For the hard-sphere matrix, the bridge functions b_{01} and b_{11} can be obtained from the equilibrium hard-sphere mixture. The function $b_b(r)$, which is used in the closure for $c_b(r)$, can be approximated in various ways. However, in our study here only the simple HNC approximation is numerically investigated for the hard-sphere matrix.

B. PY-type approximations

We now consider closures of reference Percus-Yevick (RPY) type. We have in general for this family of closures

$$c_{ij} = f_{ij} y_{ij} + d_{ij}, \tag{3.10}$$

where f_{ij} is the Mayer function and y_{ij} is the cavity function. Also, the functions $\{d_{ij}(r)\}$ are called the tail functions; they are to be approximated using the tail functions from a simpler model. The function d_{11} contains all the terms in c_b because, by definition, it contains all the terms in c_{11} that lack a Mayer bond between the roots and all contributions to c_b, by definition, have this property. We can thus incorporate the cooperative effects of the contribution (3.1) by approximating d_{11} by c_b, and using for the latter the reference system value (3.1). For many applications, it is then also natural to let $d_{01} = d_{01}^R$ and $d_{00} = d_{00}^R$ as well, where the superscript R refers to the reference system obtained by letting $\rho_1 \to 0$. This yields a version of the reference PY (RPY) approximation that seems appropriate to quenched-annealed mixtures. For this reference system, the RPY gives the result (3.1) for the function $c_b(r)$ in the random-matrix case for all ρ_1.

Let us now consider the RPY for a hard-particle matrix composed of particles similar in size to those of the fluid with $\sigma_{10} = \sigma_{11} = \sigma_{00}$. The reference system for this model is identical to the equilibrium hard-sphere fluid. To see this, note that the two annealed tracer particles do not disturb the statistics of the quenched particles they are immersed in. Also these particles are here taken to be identical in size to quenched particles. Thus, we have

$$d_{11} = d_{10} = d_{00}. \tag{3.11}$$

This gives

$$c_{11} = f_{11} y_{11} + d_{00}, \tag{3.12}$$

$$c_{10} = f_{10} y_{10} + d_{00}, \tag{3.13}$$

$$c_{00} = f_{00} y_{00}. \tag{3.14}$$

The tail function for a mixture of hard spheres can be calculated from the bridge function for this system, using the standard approximations for this purpose.

Previous simulations of this system show the usual PY approximation to be accurate through moderate fluid densities. We can partly justify this result through diagrammatic analysis of the correlation functions. The two lowest-order terms in density that appear in the expansion of c_b (and d_{11}^R) are

$$\tfrac{1}{2} \int d3d4 f_{10}(13) f_{10}(14) \rho_0(3) \rho_0(4) f_{01}(32) f_{01}(42) \tag{3.15}$$

and

$$\tfrac{1}{2} \int d3\, d4\, f_{10}(13) f_{10}(14) \rho_0(3) f_{00}(34) \rho_0(4) f_{01}(32) f_{01}(42). \tag{3.16}$$

The same near cancellation of these terms that helps account for the accuracy of the PY approximation for hard spheres at moderate densities [6] will also tend to operate in favor of the PY approximation.

By construction, the reference PY becomes increasingly accurate for low fluid-particle density. But one also expects the RPY approximation to perform better at higher fluid-particle density than the PY approximation. One sees readily by analysis of the Mayer series in the RPY approximation that the terms given by (3.15) and (3.16) are correctly included in c_b.

Finally we should mention a phenomenological approximation which we shall denote on the generalized percolation theory (GPT). If one considers h_c to represent the correlation between particles inside a pore in the matrix, one might argue that for the fluid percolating through the pores, h_c should be calculated from the total correlation function of an equilibrium fluid at an equivalent density equal to the average density of the fluid inside a pore. This can be estimated from

$$\rho_1^{eq} = \rho_1/H \tag{3.17}$$

with

$$H = \exp\left[-4\pi\rho_0\sigma_{01}^3/3\right]. \tag{3.18}$$

This approximation will prove useful for moderate to high fluid densities.

IV. NUMERICAL SOLUTION OF INTEGRAL EQUATIONS

In this section we give an algorithm for solving the ROZ equations for fluid in a quenched matrix, even at very high matrix density and/or fluid-particle density.

As a first step for the solution of the set of equations (2.3)–(2.7) these must be cast into a form suitable for numerical computation. It is convenient to express all equations in terms of short-range and well-behaved functions. A natural choice is the linear combination

$$\gamma_{\alpha\beta}(r) \equiv h_{\alpha\beta}(r) - c_{\alpha\beta}(r). \tag{4.1}$$

Solving Eqs. (2.3)–(2.7) in terms of the direct correlation functions $c_{\alpha\beta}(r)$ and using Eq. (4.1), one gets

$$\begin{aligned}
\tilde{\gamma}_{10} &= -\tilde{c}_{10} + \frac{\tilde{c}_{10}\left(1+\tilde{h}_{00}\,\rho_0\right)}{1-\tilde{c}_{11}\,\rho_1+\tilde{c}_b\,\rho_1}, \\
\tilde{\gamma}_{11} &= -\tilde{c}_{11} + \frac{\tilde{c}_{11}+\tilde{c}_{10}^2\,\rho_0+\tilde{c}_{10}^2\,\tilde{h}_{00}\,{\rho_0}^2-\rho_1\,(\tilde{c}_{11}-\tilde{c}_b\,)^2}{\left(1-\tilde{c}_{11}\,\rho_1+\tilde{c}_b\,\rho_1\right)^2}, \\
\tilde{\gamma}_b &= -\tilde{c}_b + \frac{\tilde{c}_b+\tilde{c}_{10}^2\,\rho_0+\tilde{c}_{10}^2\,\tilde{h}_{00}\,{\rho_0}^2}{\left(1-\tilde{c}_{11}\,\rho_1+\tilde{c}_b\,\rho_1\right)^2}.
\end{aligned} \tag{4.2}$$

These expressions can be rewritten in a form more suitable for numerical computation by using the functions

$$\begin{aligned}
\tilde{\Gamma}_{\alpha\beta}(k_j) &= k_j\tilde{\gamma}_{\alpha\beta}(k_j), \\
\tilde{H}_{\alpha\beta}(k_j) &= k_j\tilde{h}_{\alpha\beta}(k_j), \\
\tilde{C}_{\alpha\beta}(k_j) &= k_j\tilde{c}_{\alpha\beta}(k_j).
\end{aligned} \tag{4.3}$$

Here the tilde atop a quantity denotes its Fourier transform. Also, we adopt the notation that capitalized quantities (like $\tilde{C}$, e.g.) are related to the corresponding uncapitalized quantities (like $\tilde{c}$) by a factor of k and correspondingly for the functions in r space. We calculate Fourier transforms on a discrete mesh of N points with spacing Δk, where we choose $\Delta k\Delta x = \pi/N$. This guarantees orthogonality between backward and forward Fourier transforms. We employ discretized Fourier transforms which can be written, e.g.,

$$\begin{aligned}
\tilde{\Gamma}_{\alpha\beta}(k_j) &= 4\pi\Delta r\sum_i \Gamma_{\alpha\beta}(r_i)\sin\frac{\pi ij}{N}, \\
\Gamma_{\alpha\beta}(r_i) &= \frac{\Delta k}{2\pi^2}\sum_j \tilde{\Gamma}_{\alpha\beta}(k_j)\sin\frac{\pi ij}{N}.
\end{aligned} \tag{4.4}$$

The equations (4.2) then become

$$\begin{aligned}
\tilde{\Gamma}_{10}(k_j) &= -\tilde{C}_{10}(k_j) + \frac{\tilde{C}_{10}(k_j)\,\chi(k_j)}{k_j-\tilde{C}_{11}(k_j)\,\rho_1+\tilde{C}_b(k_j)\,\rho_1}, \\
\tilde{\Gamma}_{11}(k_j) &= -\tilde{C}_{11}(k_j) + \frac{k_j^2\tilde{C}_{11}(k_j)+\rho_0\tilde{C}_{10}(k_j)^2\chi(k_j)-k_j\rho_1\left[\tilde{C}_{11}(k_j)-\tilde{C}_b(k_j)\right]^2}{\left[k_j-\tilde{C}_{11}(k_j)\,\rho_1+\tilde{C}_b(k_j)\,\rho_1\right]^2}, \\
\tilde{\Gamma}_b(k_j) &= -\tilde{C}_b(k_j) + \frac{k_j^2\tilde{C}_b(k_j)+\rho_0\tilde{C}_{10}(k_j)^2\chi(k_j)}{\left[k_j-\tilde{C}_{11}(k_j)\,\rho_1+\tilde{C}_b(k_j)\,\rho_1\right]^2}
\end{aligned} \tag{4.5}$$

with $\chi(k_j) = k_j + \rho_0\tilde{H}_{00}(k_j)$.

We need to supplement the Ornstein-Zernike equations (4.2) by providing additional relations, usually called closure relations, between the $\{\Gamma_{ij}\}$ and the $\{C_{ij}\}$. We will specialize the closures developed in Sec. III to the systems studied here.

(1) *Reference Percus-Yevick closures.* If the reference system is chosen to be an ideal gas, the standard or naive PY approximation results. If the reference system of this paper is used to evaluate (3.10) the results, expressed in the notation of this section, are

$$C_{10}(r) = \begin{cases} -r-\Gamma_{10}(r) & \text{if } r<\sigma_{10} \\ C_{10}^R & \text{if } r\geq\sigma_{10}, \end{cases} \tag{4.6}$$

and

$$C_{11}(r) = \begin{cases} -r-\Gamma_{11}(r) & \text{if } r<\sigma_{11} \\ C_{11}^R & \text{if } r\geq\sigma_{11}. \end{cases} \tag{4.7}$$

The first condition in each of the two braces in (4.6) and (4.7), the "short-range" condition, is exact; it simply enforces the excluded-volume constraints on $H_{10}(r)$ and $H_{11}(r)$. The second condition of each pair sets the functions $C_{10}(r)$, $C_{10}(r)$, respectively, equal to their values in the reference system. Setting both reference functions equal to zero gives the standard PY approximation, to which the MG approximation reduces for hard-sphere systems.

In the random-matrix case, the reference system de-

fined by the $\rho \to 0$ limit yields $C_{10}(r) = 0$ and $C_{11}(r) = rc_b(r)$ with $c_b(r)$ given by (3.1). For hard-sphere potentials one obtains

$$O(r) = \frac{4\pi}{3}[\sigma_{01}^3 - \tfrac{3}{4}\sigma_{01}^2 r + \tfrac{1}{16}r^3]. \tag{4.8}$$

In the case of a hard-sphere matrix, the RPY approximation can be expressed as follows:

$$C_{\alpha\beta}(r) = \begin{cases} -r - \Gamma_{\alpha\beta}(r) & \text{if } r < \sigma_{\alpha\beta} \\ r d_{00}(r) & \text{if } r \geq \sigma_{\alpha\beta}, \end{cases} \tag{4.9}$$

where (α, β) is $(1,0)$ or $(1,1)$, and

$$C_b(r) = r d_{00}(r) = \begin{cases} r[y_{00}(r) + c_{00}(r)] & \text{if } r < \sigma_{11} \\ r c_{00}(r) & \text{if } r \geq \sigma_{11}, \end{cases} \tag{4.10}$$

where $c_{00}(r)$ and $y_{00}(r)$ are pure hard-sphere quantities that can be obtained by solving the Ornstein-Zernike equation using as input the Verlet-Weis parametrization of the radial distribution function [12] and the Henderson-Grundke parametrization [13] of $y(r) = \exp[\beta u(r)]g(r)$.

(2) *Reference hypernetted-chain closure.* If the reference system is chosen to be an ideal gas, the standard or naive HNC approximation results. If the reference system of this paper is used to evaluate the general reference HNC scheme (3.7) the result is

$$C_{\alpha\beta}(r) = \begin{cases} -r - \Gamma_{\alpha\beta}(r) & \text{if } r < \sigma_{\alpha\beta} \\ r \exp\left[\Gamma_{\alpha\beta}(r)/r\right] - r - \Gamma_{\alpha\beta}(r) & \text{if } r \geq \sigma_{\alpha\beta}, \end{cases} \tag{4.11}$$

where (α, β) is $(1,0)$ or $(1,1)$, and

$$C_b(r) = r \exp\left[\Gamma_b(r)/r\right] - r - \Gamma_b(r). \tag{4.12}$$

At low densities and for PY-type approximations these equations can be solved by simple substitution methods (convergence might be speeded up by using Broyles mixing iterates procedure). However, at higher densities of fluid and/or matrix particles, and in particular when solving the HNC closure, a more sophisticated numerical procedure is required. The method we have used here belongs to the family of hybrid Newton-Raphson procedures developed by Gillan [14], and it is in fact an extension of previous work by Labik, Malijevsky and Vonka [15] and by two of the authors in collaboration with Høye [16]. The procedure can be sketched as follows:

(1) Set the difference functions

$$\begin{aligned} \Phi_{10}(k_j) &= \tilde{\Gamma}_{10}(k_j) - F_{10}(k_j), \\ \Phi_{11}(k_j) &= \tilde{\Gamma}_{11}(k_j) - F_{11}(k_j), \\ \Phi_b(k_j) &= \tilde{\Gamma}_b(k_j) - F_b(k_j) \end{aligned} \tag{4.13}$$

equal to zero in a large domain of k space defined by $k_j, j = 1, \ldots, M$. Here by $F_{\alpha\beta}$ we denote the algebraic expressions on the right-hand side of Eqs. (4.5).

(2) Given a first estimate of the $\Gamma_{\alpha\beta}$ (a PY solution for an equilibrium mixture or even for two noninteracting fluids will suffice in this respect) one gets $C_{\alpha\beta}(r)$ from the desired closure relation

$$C_{\alpha\beta}(r) = F[\Gamma_{\alpha\beta}(r)]$$

where $F[\cdots]$ stands for any direct functional relation (PY, HNC,...).

(3) Once Fourier transformed, both $C_{\alpha\beta}$ and $\Gamma_{\alpha\beta}$, one can perform a first-order Taylor-series expansion around the initial estimate (which we will denote by a zero superscript)

$$\tilde{C}_{\alpha\beta}(k_j) = \tilde{C}^0_{\alpha\beta}(k_j) + \sum_{l=1}^{M} \mathcal{C}_{\alpha\beta;jl} \left[\tilde{\Gamma}_{\alpha\beta}(k_l) - \tilde{\Gamma}^0_{\alpha\beta}(k_l)\right], \tag{4.14}$$

where

$$\mathcal{C}_{\alpha\beta;jl} = D_{\alpha\beta}(|j-l|) - D_{\alpha\beta}(j+l) \tag{4.15}$$

and

$$D_{\alpha\beta}(l) = \frac{1}{N}\sum_i \left(\frac{\partial C_{\alpha\beta}(r)}{\partial \Gamma_{\alpha\beta}(r)}\right)_r \cos(\pi i l). \tag{4.16}$$

The derivative in this latter expression depends on the closure to be used. For PY-type equations we have

$$\left(\frac{\partial C_{\alpha\beta}(r)}{\partial \Gamma_{\alpha\beta}(r)}\right)_r = \begin{cases} -1 & \text{if } r < \sigma_{\alpha\beta} \\ 0 & \text{if } r \geq \sigma_{\alpha\beta} \end{cases} \tag{4.17}$$

and $\partial C_b / \partial \Gamma_b = 0$. The HNC closure yields

$$\left(\frac{\partial C_{\alpha\beta}(r)}{\partial \Gamma_{\alpha\beta}(r)}\right)_r = h_{\alpha\beta}(r). \tag{4.18}$$

Expression (4.16) above can easily be evaluated by means of standard fast Fourier transforms.

(4) The problem now reduces to solving Eqs. (4.13) with Eq. (4.14) inserted to obtain the new $\Gamma_{\alpha\beta}$. This can be achieved by means of the Newton-Raphson method

$$\Delta\tilde{\Gamma}_{\alpha\beta}(k_j) = -\sum_{\mu,\nu,l} \left[\mathbf{J}^{-1}\right]_{\alpha\beta\mu\nu;jl} \Phi_{\alpha\beta}(k_l) \tag{4.19}$$

and a new Newton-Raphson estimate is obtained every time Eq. (4.19) is iterated by

$$\tilde{\Gamma}^{n+1}_{\alpha\beta} = \tilde{\Gamma}^n_{\alpha\beta} + \Delta\tilde{\Gamma}_{\alpha\beta}.$$

The Jacobian elements in Eq. (4.19) are given by

$$J_{\alpha\beta\mu\nu;jl} = \delta_{\alpha\mu}\delta_{\beta\nu}\delta_{jl} - \frac{d\tilde{\Gamma}_{\alpha\beta}(k_j)}{d\tilde{C}_{\mu\nu}(k_j)} \mathcal{C}_{\mu\nu;jl}. \tag{4.20}$$

Explicit expressions for the Jacobian elements derived from the Eqs. (4.5) can be found in the Appendix.

(5) Once a converged solution from the Newton-Raphson is obtained for $\tilde{\Gamma}_{\alpha\beta}(k_j)$ (in the range $j = 1, \ldots, M$ one performs a direct iteration on Eqs. (4.5) for $j = M+1, \ldots, N$ and the result is combined with the output of the Newton-Raphson method to yield a complete new estimate for $\Gamma_{\alpha\beta}(r)$ and one iterates from step 2 until convergence is achieved. We assume convergence when

$$\xi_{\alpha\beta} = \sqrt{\sum_i \left[\Gamma^{new}_{\alpha\beta}(r) - \Gamma^{old}_{\alpha\beta}(x)\right]^2} < 10^{-5}$$

for all values of $\alpha\beta$.

TABLE I. Technical details of the simulation conditions for the random obstacle system ($\sigma_{00} = 0, \sigma_{10} = 2.5, \sigma_{11} = 1$).

ρ_0	N_0	ρ_1	$\bar{N}_1$	No. of moves	No. of matrix configurations
0.05	333	0.0257 ± 0.0005	171	1.5×10^6	30
0.01	80	0.0258 ± 0.0001	206	2.0×10^6	40
0.01	20	0.4180 ± 0.0020	836	7.0×10^6	40
0.02	38	0.1900 ± 0.0020	361	2.0×10^6	30
0.02	380	0.0124 ± 0.0001	235	1.3×10^6	40

The MG equations follow automatically from the ROZ equations when the PY approximation is made, and they do not pose special problems. We note in passing that contrary to what was found in previous works on equations of Ornstein-Zernike type [16, 17], here the Jacobian matrix must unavoidably be recomputed each iteration, otherwise the system becomes unstable.

V. NUMERICAL RESULTS

In this section we present the results of solving the ROZ equations, in the various approximations of Sec. III, for the two models of quenched media studied in this paper. We compare these to detailed simulations of these models, which supplement earlier simulation results by Fanti, Glandt, and Madden [4].

The simulations were performed in a cubic box of fixed volume V with periodic boundary conditions using the Monte Carlo method. We choose to use a grand canonical Monte Carlo (GCMC) sampling technique [18, 19] which is convenient when the volume accessible to the fluid particles consists of disjoint or porously connected areas. The detailed procedure was as follows. First a matrix configuration is constructed. For the quenched hard-sphere case matrix configurations consisted of independent equilibrium configurations taken from a trajectory in phase space sampled from the grand canonical ensemble at an average density $\rho_0 = \bar{N}_0/V$ ($\bar{N}_0$ is the average number of matrix particles). Different configurations were typically separated by 2000 attempted displacements per particle. In the random-matrix case a matrix configuration was obtained by simply inserting N_0 possibly overlapping spheres in the volume V. Next, an arbitrary number of fluid particles was inserted into the matrix by "brute force," i.e., by randomly choosing a position in the volume and assuring that the inserted particle did not overlap with either the matrix or the other fluid particles. The fluid system was then equilibrated at an average density $\rho_1 = \bar{N}_1/V$ ($\bar{N}_1$ is the average number of fluid particles) using GCMC sampling and an equilibrium trajectory in phase space was generated along which the fluid-fluid pair distribution function was calculated. For specified densities ρ_0 and ρ_1, the number of matrix particles N_0 was generally chosen so that the number of fluid particles was at least of the order of 200. The precise characteristics of the various MC runs are summarized in Tables I and II. The GCMC method involves three types of moves:

(1) displacement of a particle,
(2) destruction of a particle,
(3) creation of a particle at a random position in the medium.

Attempts of displacement, creation, and destruction of a particle were performed in cycles. The decisions for acceptance of the three types of steps were determined from the conditions [19]

$$\text{displacement:}\quad e^{-\Delta U/kT} \geq \xi,$$

$$\text{creation:}\quad \left[1 + \frac{N_1 + 1}{zV} e^{\Delta U/kT}\right]^{-1} \geq \xi,$$

$$\text{destruction:}\quad \left[1 + \frac{zV}{N_1} e^{\Delta U/kT}\right]^{-1} \geq \xi,$$

where ΔU is the change in energy involved in the proposed step (note that $\Delta U = \infty$ if there is overlap between two particles, and $\Delta U = 0$ if there is not), $z = \exp(\mu/kT)/\Lambda^3$ is the activity (μ is the chemical potential, k is the Boltzmann constant, T is temperature, Λ is the de Broglie wavelength), N_1 is the number of fluid particles prior to the attempted move, and ξ is a random number in the interval $(0, 1)$.

As GCMC are performed at a fixed chemical potential and the latter is unknown for the present system, μ was varied until the desired fluid density was obtained. For the densities considered in the present study an insertion method based on a randomly selected point turned out to be sufficient. At higher densities a cavity-biased insertion procedure could be advantageously applied [20–22].

We first discuss the results for fluid in a matrix made of freely overlapping obstacles. (For brevity we will term

TABLE II. Technical details of the simulation conditions for the quenched hard-sphere system ($\sigma_{00} = \sigma_{10} = \sigma_{11} = 1$).

ρ_0	$\bar{N}_0$	ρ_1	$\bar{N}_1$	No. of moves	No. of matrix configurations
0.30	256	0.299 ± 0.003	256	1.6×10^6	12
0.609	507	0.0996	83	0.15×10^6	30

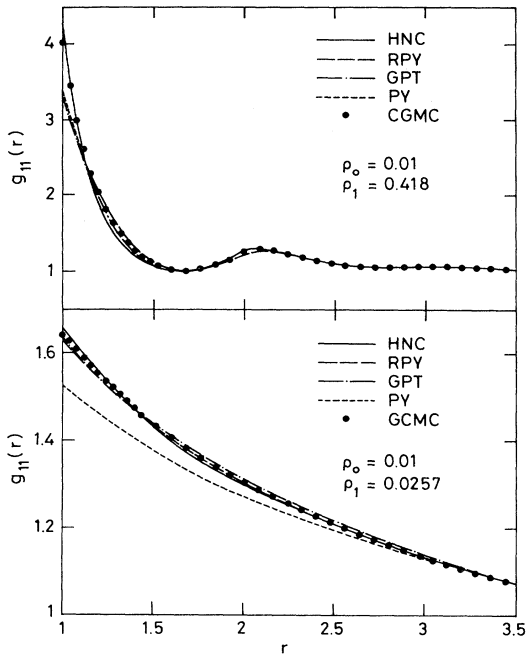

FIG. 1. Fluid-fluid pair-distribution function $g_{11}(r)$ for a random-matrix system at $\rho_0 = 0.01$ (high porosity, $H = 0.52$) for high and low fluid density (upper and lower figures, respectively). Solid circles denote GCMC results. In this model $\sigma_{11} = 1$, $\sigma_{10} = 2.5$, and $\sigma_{00} = 0$. The HNC, RPY, and GPT approximations are versions introduced by Given and Stell in Refs. [1], [5], and [7] in the context of their ROZ equations and described here in the text. The PY approximation was first used for this system in [4].

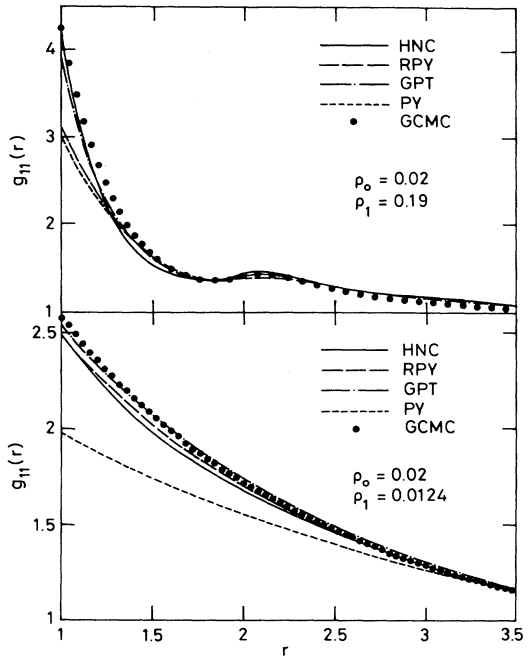

FIG. 3. Fluid-fluid pair-distribution function $g_{11}(r)$ for a random-matrix system at $\rho_0 = 0.02$ (low porosity, $H = 0.27$) for high and low fluid density (upper and lower figures, respectively). Solid circles denote GCMC results. In this model $\sigma_{11} = 1$, $\sigma_{10} = 2.5$, and $\sigma_{00} = 0$. Notation as in Fig. 1.

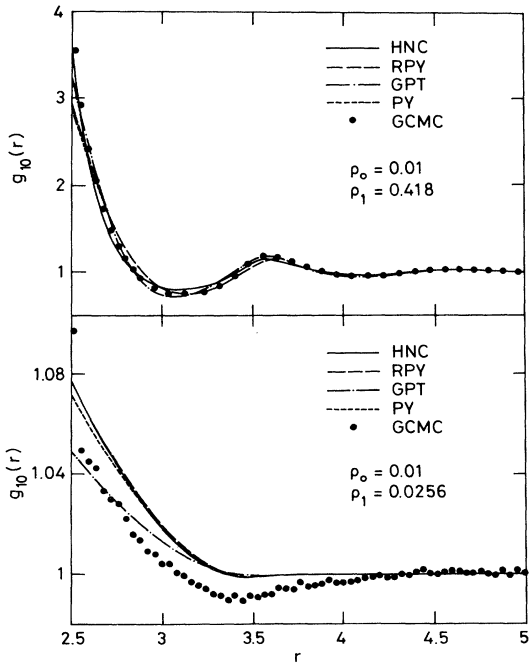

FIG. 2. Fluid-matrix distribution function for the random-matrix system. Densities, geometric parameters, and notation as in Fig. 1.

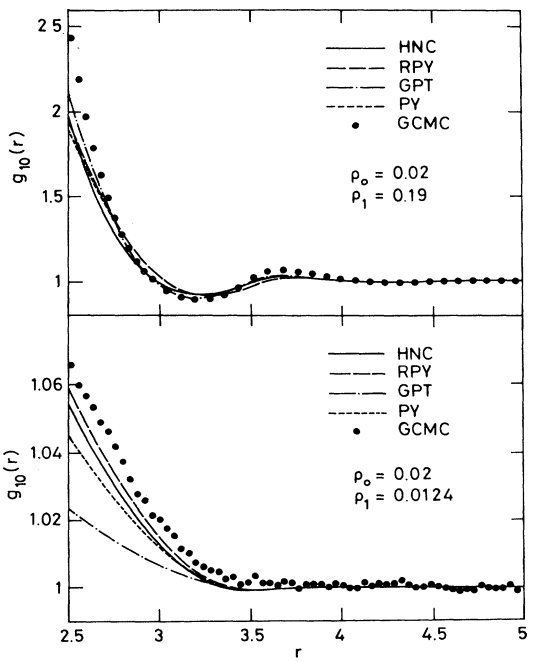

FIG. 4. Fluid-matrix distribution function for the random-matrix system. Densities, geometric parameters, and notation as in Fig. 3.

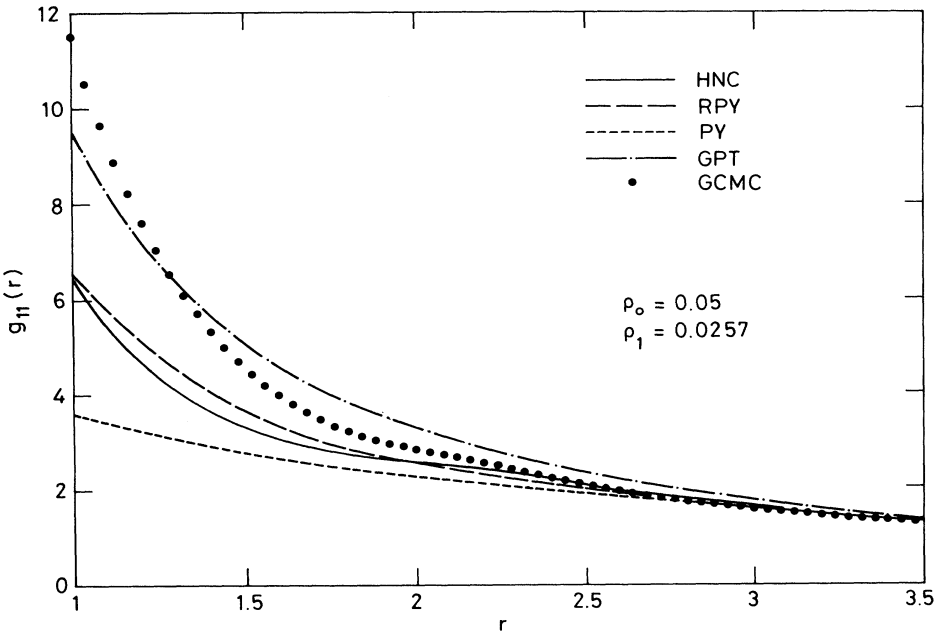

FIG. 5. Fluid-fluid distribution function for a system of extremely high matrix density ($\rho_0 = 0.05, H = 0.03$) and low fluid density ($\rho_1 = 0.0257$). Notation as in Fig. 1.

this a "random matrix"; our model for a consolidated matrix composed of nonoverlapping particles will be called a "hard-sphere matrix.") The random-matrix model was studied by Fanti, Glandt, and Madden [4] using Monte Carlo simulation for fairly low densities of both fluid particles and matrix particles. In this regime they found that the PY approximation gives good agreement with simulation. We have reproduced the results they report. We have also obtained simulation results at other combinations of fluid and matrix densities for this system which we present here. The ratio between fluid-fluid and fluid-matrix interaction ranges is $\sigma_{01}/\sigma_{11} = 2.5$ in our random-matrix comparisons. The ratio was chosen to be considerably greater than one in order to bring out the effect of the c_b contribution to c_{11} in the ROZ equations. This contribution, which is missing in the PY approximation, increases rapidly with increasing σ_{10}/σ_{11}. Fluid-fluid and fluid-matrix correlation functions are found in Figs. 1–4 for high and low matrix porosity and high and low fluid densities. The porosity of the matrix is described by Henry's constant, defined by Eq. (3.18), which accounts for the amount of space available in the matrix for insertion of a fluid particle.

Among the approximations we have considered for the random-matrix case, the HNC appears to be best in an overall way over a considerable range of conditions. How-

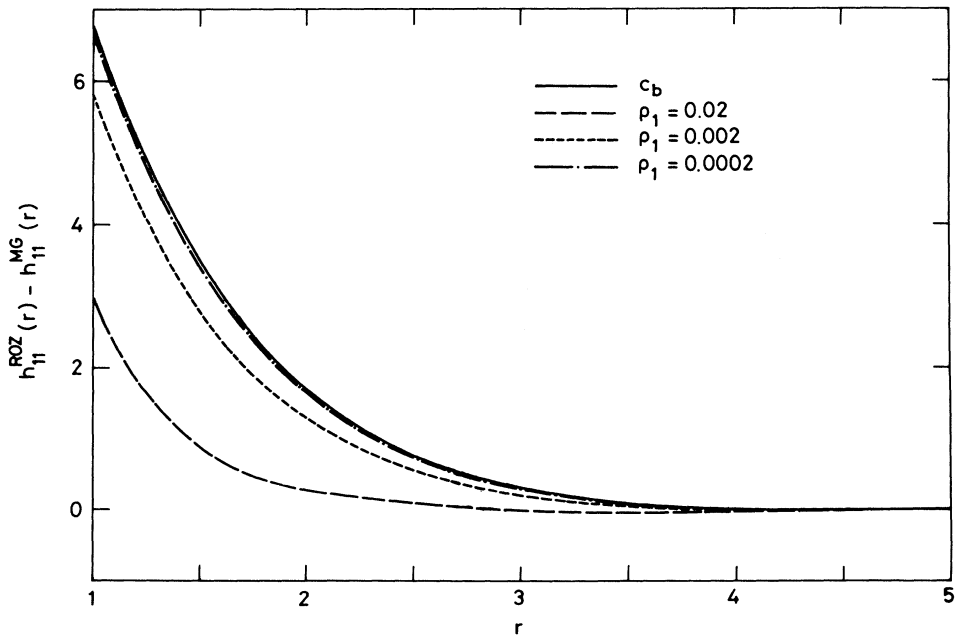

FIG. 6. Difference function $h_{11}^{ROZ}(r) - h_{11}^{MG}(r)$ for a random-matrix system at $\rho_0 = 0.05$ (extremely low porosity, $H = 0.03$) and for various fluid densities, ρ_1. The solid line denotes $c_b(r)$ obtained from Eq. (3.1).

ever, it leaves room for substantial improvement as our Figs. 1–5 make clear.

At high fluid densities (exemplified by the state with $\rho_1 = 0.418$ and $\rho_0 = 0.01$) the HNC and GPT approximations are very similar, yielding g_{11} and g_{10} values that are closer to simulation results at and near the contact value of $r = 1$ than the RPY and PY values, which are very similar to each other for this state and are too low near contact (see Figs. 1 and 2). These trends persist for $g_{11}(r)$ at a state of moderate matrix density and moderate fluid density ($\rho_0 = 0.02$, $\rho_1 = 0.19$), at which all the approximations for $g_{10}(r)$ became rather similar, and rather poor (see Figs. 3 and 4). At the high and moderate fluid densities, the too-low contact values of the PY and RPY results are partly offset by their somewhat more faithful treatment of the bowl of the first minimum of g_{11} and g_{10} (see Figs. 1–4).

At lower fluid densities and moderate matrix densities (exemplified by the results shown for $\rho_0 = 0.02$, $\rho_1 = 0.0124$ and $\rho_0 = 0.01$, $\rho_1 = 0.0257$) the RPY and PY results are quite different from one another, with the RPY results satisfactory and the PY results poor. For these states of moderate matrix densitx and low fluid density, the RPY and HNC results are nearly coincident. The HNC result for g_{11} is almost exact, except for g_{11} values at and near contact that are slightly high (see Figs. 1–4).

For a system with an extremely high matrix density ($\rho_0 = 0.05$ at $\rho_1 = 0.0257$), the GPT is relatively more accurate than any of the other approximations studied here, but it is not of high quantitative accuracy.

The PY results are in general not quantitatively satisfactory for the rather large σ_{10}/σ_{11} ratio of 2.5 we consider here. They are at their best in the moderate to high fluid density range with moderate matrix density, for which the PY and RPY results are nearly indistinguishable. A simple argument illuminates the relation between the PY and RPY closures for the random-matrix model. The two terms which are present in the ROZ equation (2.5) for $h_{11}(r)$, but absent in the corresponding equation (20) of Madden and Glandt [4], are

$$h_{11}^{\mathrm{ROZ}} - h_{11}^{\mathrm{MG}} = c_b + \rho_1 c_b \otimes h_c, \tag{5.1}$$

where the $\otimes$ denotes a convolution. Explicit numerical evaluation of this difference for a moderate-density matrix formed by randomly overlapping particles shows that the second term is much smaller than the first at low fluid densities, while at moderate fluid densities the two terms approximately cancel (see Fig. 6). Also, at low fluid densities, the term c_b dominates all the other terms on the right-hand side of (2.5). This explains why the "ideal-gas" result (3.1) gives a good approximation for this quantity at low fluid density.

Finally we consider the model of a fluid adsorbed in a hard-particle matrix. Distribution functions for this system in the simple equal-diameter case are shown in Figs. 7 and 8 for high and low porosities. Overall, the RPY, as formulated by Eqs. (3.12)–(3.14) for nonpenetrable matrices, proves to be the best approximation among those we considered. The PY approximation for $g_{11}(r)$ is adequate at low to moderate fluid and matrix densities (the

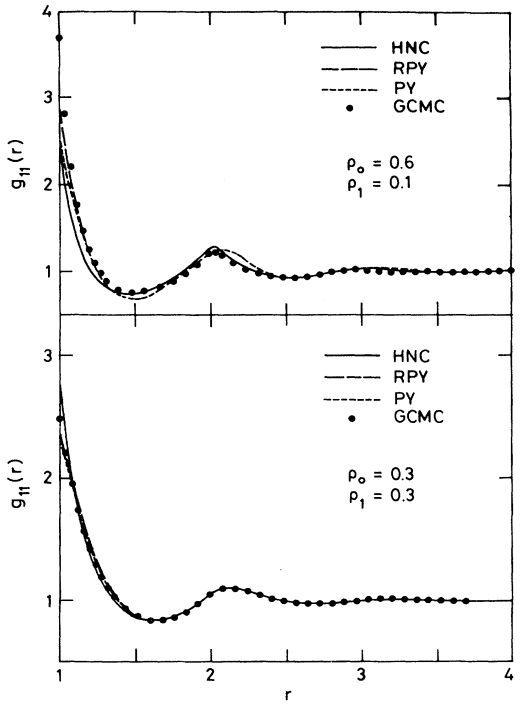

FIG. 7. Fluid-fluid distribution function for the quenched hard-sphere matrix system. In this model $\sigma_{11} = \sigma_{10} = \sigma_{00} = 1$ and $\rho_0 = 0.6$, $\rho_1 = 0.1$ (upper figure) and $\rho_0 = 0.3$, $\rho_1 = 0.3$ (lower figure). Notation as in Fig. 1.

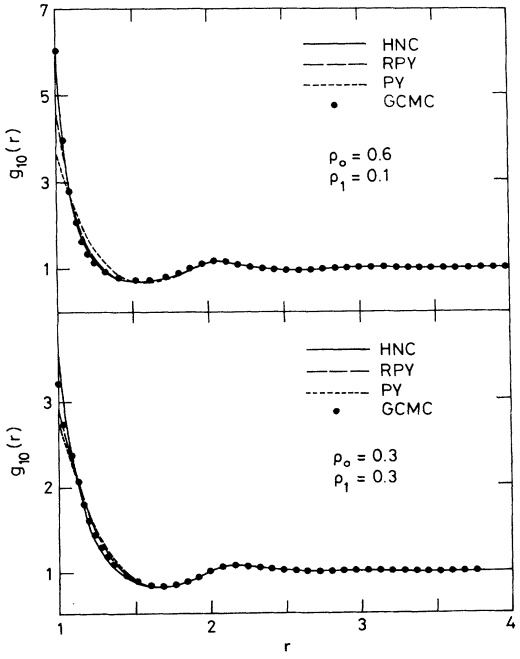

FIG. 8. Fluid-matrix distribution function for the quenched hard-sphere matrix system. Densities, geometric parameters, and notation as in Fig. 7.

latter exemplified by our $\rho_0 = \rho_1 = 0.3$ state), but for our high matrix-density state ($\rho_0 = 0.6$, $\rho_1 = 0.1$) it is not quantitatively accurate. The PY $g_{10}(r)$ results are too low near contact, $r = 1$, where they underestimate $g_{10}(r)$ considerably. The RPY results substantially correct these deficiencies. In particular, they give higher $g(r)$ values near contact, but still not high enough to match the simulation results at contact. The HNC results for $g_{11}(r)$ and $g_{10}(r)$ are in general not as good as the RPY results, except for the $g_{01}(r)$ result at $\rho_0 = 0.6$, $\rho_1 = 0.1$, which is our best result for $g_{10}(r)$ at this high matrix-density state.

ACKNOWLEDGMENTS

E.L. would like to acknowledge the Dirección General de Investigación Científica y Técnica which supported his stay at the State University of New York at Stony Brook with a grant. J.G. is grateful to the National Science Foundation for their support of this work. G.S. gratefully acknowledges financial support from the Division of Chemical Sciences, Office of Basic Energy Sciences, Office of Energy Research, U.S. Department of Energy. The research of the Stony Brook group was conducted using the Cornell National Supercomputer Facility, a resource of the Center for Theory and Simulations in Science and Engineering (Cornell Theory Center), which receives major funding from the National Science Foundation and IBM Corporation, with additional support from New York State and members of the Corporate Research Institute.

APPENDIX: COMPONENTS OF THE JACOBIAN MATRIX FOR THE ROZ EQUATIONS

For simplicity we define

$$F_{\alpha\beta\mu\nu} = \frac{d\tilde{\Gamma}_{\alpha\beta}(k_j)}{d\tilde{C}_{\mu\nu}(k_j)} \tag{A1}$$

and thus the only required elements of the Jacobian can be computed from the following expressions:

$$\begin{aligned}
F_{1010} &= \frac{k + \tilde{H}_{00}\,\rho_0}{k - \tilde{C}_{11}\,\rho_1 + \tilde{C}_b\,\rho_1} - 1, \\
F_{1011} &= \frac{\tilde{C}_{10}\,(k + \tilde{H}_{00}\,\rho_0)\rho_1}{\left(k - \tilde{C}_{11}\,\rho_1 + \tilde{C}_b\,\rho_1\right)^2}, \\
F_{1012} &= -\frac{\tilde{C}_{10}\,(k + \tilde{H}_{00}\,\rho_0)\rho_1}{\left(k - \tilde{C}_{11}\,\rho_1 + \tilde{C}_b\,\rho_1\right)^2}, \\
F_{1110} &= \frac{2\,\tilde{C}_{10}\,\rho_0\,(k + \tilde{H}_{00}\,\rho_0)}{\left(k - \tilde{C}_{11}\,\rho_1 + \tilde{C}_b\,\rho_1\right)^2}, \\
F_{1111} &= \frac{k^3 - \tilde{C}_{11}\,k^2\,\rho_1 + 3\,\tilde{C}_b\,k^2\,\rho_1 + 2\,\tilde{C}_{10}^2\rho_0\,\rho_1(k + \tilde{H}_{00}\,\rho_0)}{\left(k - \tilde{C}_{11}\,\rho_1 + \tilde{C}_b\,\rho_1\right)^3} - 1, \\
F_{1112} &= \frac{2\,[\tilde{C}_b\,k^2 + \tilde{C}_{10}^2\,\rho_0(k + \tilde{H}_{00}\,\rho_0)]\,\rho_1}{\left(-k + \tilde{C}_{11}\,\rho_1 - \tilde{C}_b\,\rho_1\right)^3}, \\
F_{1210} &= \frac{2\,\tilde{C}_{10}\,\rho_0\,(k + \tilde{H}_{00}\,\rho_0)}{\left(k - \tilde{C}_{11}\,\rho_1 + \tilde{C}_b\,\rho_1\right)^2}, \\
F_{1211} &= \frac{2\,[\tilde{C}_b\,k^2 + \tilde{C}_{10}^2\rho_0(k + \tilde{H}_{00}\,\rho_0)]\,\rho_1}{\left(k - \tilde{C}_{11}\,\rho_1 + \tilde{C}_b\,\rho_1\right)^3}, \\
F_{1212} &= \frac{k^3 - \tilde{C}_{11}\,k^2\,\rho_1 - \tilde{C}_b\,k^2\,\rho_1 - 2\,\tilde{C}_{10}^2\rho_0\,\rho_1(k + \tilde{H}_{00}\rho_0)}{\left(k - \tilde{C}_{11}\,\rho_1 + \tilde{C}_b\,\rho_1\right)^3} - 1
\end{aligned} \tag{A2}$$

inserted in Eq. (A1) and this in Eq. (4.20). Note that in PY-type closures, the fact that $dC_b/d\Gamma_b = 0$ means that all elements $J_{1212;kl} = \delta_{kl}$ and all the remaining Jacobian terms in which the replica interaction is involved simply vanish. This implies that the NR strategy has to be applied only to the functions with subscripts 10 and 11 since these are completely independent of $\tilde{\Gamma}_b$ and C_b and will remain fixed through the iteration procedure.

* Permanent address: Instituto de Química Física Rocasolano, CSIC, Serrano 119, E-28006 Madrid, and Depto. Química Física I, U. Complutense, E-28040 Madrid, Spain.

† Permanent address: Thermophysics Division, NIST, Gaithersburg, MD 20899.

[1] J.A. Given and G. Stell, in the *XVIth International Workshop on Condensed-Matter Theories, San Juan,*

Puerto Rico, 1992 (Plenum, New York, 1993).
[2] W.G. Madden and E.D. Glandt, J. Stat. Phys. **51**, 537 (1988).
[3] W.G. Madden, J. Chem. Phys. **96**, 5422 (1992).
[4] L.A. Fanti, E.D. Glandt, and W.G. Madden, J. Chem. Phys. **93**, 5945 (1990).
[5] J.A. Given and G. Stell, J. Chem. Phys. **97**, 4573 (1992).
[6] D. Chandler, J. Phys. B: Condensed Matter, **42**, F1 (1991).
[7] J.A. Given and G. Stell, State University of New York at Stony Brook College of Engineering and Applied Sciences Report No. 640, 1992.
[8] J.A. Given, Phys. Rev. A **45**, 816 (1992).
[9] B. Widom and J.S. Rowlinson, J. Chem. Phys. **52**, 1670 (1970).
[10] See, e.g., C. Bruin, Physica **72**, 261 (1974).
[11] J.A. Given and G. Stell, J. Chem. Phys. **94**, 3060 (1991).
[12] L. Verlet and J.J. Weis, Phys. Rev. A **5**, 939 (1972).
[13] D. Henderson and E.W. Grundke, J. Chem. Phys. **63**, 601 (1975).
[14] M.J. Gillan, Mol. Phys. **49**, 421 (1983).
[15] S. Labik, A. Malijevsky, and P. Vonka, Mol. Phys. **56**, 709 (1985).
[16] J.S. Høye, E. Lomba, and G. Stell, Mol. Phys. **75**, 1217 (1992).
[17] M. Kinoshita and M. Harada, Mol. Phys. **65**, 599 (1988).
[18] G.E. Norman and V.S. Filinov, High. Temp. **7**, 216 (1969).
[19] M.P. Allen and D.J. Tildesley, *Computer Simulation of Liquids* (Clarendon, Oxford, 1982).
[20] M. Mezei, Mol. Phys. **40**, 901 (1980); **61**, 565 (1987).
[21] I. Ruff, A Baranyai, G. Palinkas, and K. Heinzinger, J. Chem. Phys. **85**, 2169 (1986).
[22] G.L. Deitrick, L.E. Scriven, and H.T. Davis, J. Chem. Phys. **90**, 2370 (1989).